Caseahomopene A, a ring-expanded homotriterpenoid from *Casearia kurzii* showing anti-inflammatory activities *in vitro* and *in vivo*

Lijun An [a,1], Jun Ma [a,1], Xueyuan Yang [a,1], Yue Liang [a,1], Huimei Wang [a], Muhetaer Tuerhong [b], Namrita Lall [c], Munira Abudukeremu [b], Yi Zhang [d], Dongho Lee [e], Jing Xu [a,f,*], Xiaohui Wu [g,*], and Yuanqiang Guo [a,*]

[a] *State Key Laboratory of Medicinal Chemical Biology, College of Pharmacy, and Tianjin Key Laboratory of Molecular Drug Research, Nankai University, Tianjin 300350, People's Republic of China*

[b] *College of Chemistry and Environmental Sciences, Kashgar University, Kashgar 844000, People's Republic of China*

[c] *Department of Plant and Soil Sciences, University of Pretoria, Pretoria 0002, South Africa*

[d] *Tianjin State Key Laboratory of Modern Chinese Medicine, Tianjin Key Laboratory of TCM Chemistry and Analysis, and Institute of Traditional Chinese Medicine, Tianjin University of Traditional Chinese Medicine, Tianjin 300193, People's Republic of China*

[e] *College of Life Sciences and Biotechnology, Korea University, Seoul 02841, Republic of Korea*

[f] *State Key Laboratory of Bioactive Substance and Function of Natural Medicines, Institute of Materia Medica, Chinese Academy of Medical Sciences and Peking Union Medical College, Beijing 100050, People's Republic of China*

[g] *College of Pharmacy, Tianjin Medical University, Tianjin 300070, China*

*Corresponding authors. Tel/fax: +86-22-23502595; E-mail addresses: xujing611@nankai.edu.cn (J. Xu); longhui804@163.com (X. Wu); victgyq@nankai.edu.cn (Y. Guo)

[1] These authors contributed equally to this work.

Highlights

• A rare homotriterpenoid was isolated from *Casearia kurzii*.

• The structure was elucidated by NMR data and X-ray diffraction analysis.

• The anti-inflammatory activities were investigated using cell and zebrafish models.

• Compound **1** showed anti-inflammatory effects *in vitro* and *in vivo*.

• The anti-inflammatory mechanism of **1** was explored.

Abstract

Caseahomopene A (**1**), a rare natural product with a ring-expanded homotriterpenoid skeleton, was isolated from the leaves of *Casearia kurzii*. The structure including the absolute configuration was determined by spectroscopic data and X-ray crystallography analysis. Compound **1** showed anti-inflammatory effects *in vitro* and *in vivo* using LPS-stimulated cell and zebrafish model. As a potential anti-inflammatory agent, the anti-inflammatory mechanism of **1** was also investigated.

Keywords: Homotriterpenoid; Anti-inflammation; Zebrafish model; Molecular docking; *Casearia kurzii*

Graphical abstract

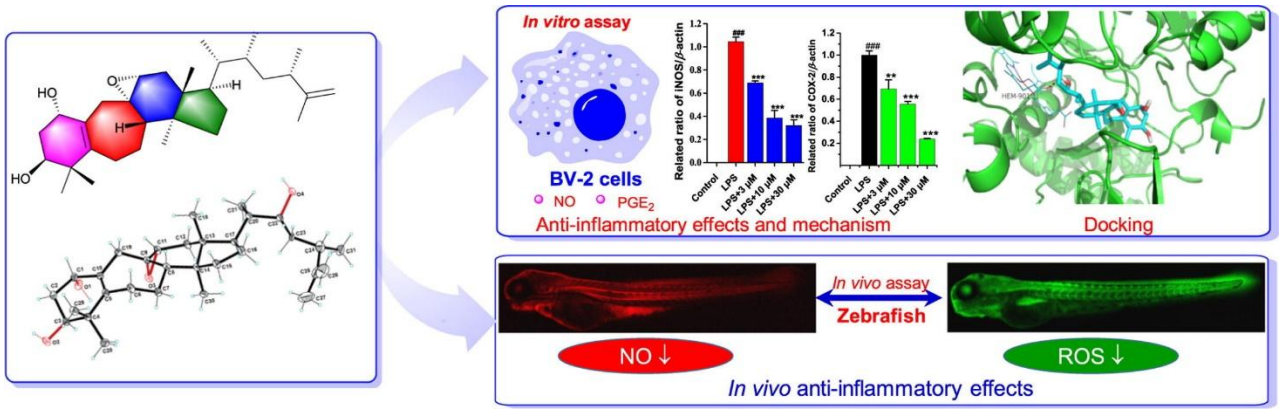

Keywords: Homotriterpenoid, Anti-inflammation, Zebrafish model, Molecular docking, *Casearia kurzii*

1. Introduction

A growing number of studies have shown that inflammation, especially chronic inflammation, is intimately related to the pathogenesis of atherosclerosis [1], obesity and related metabolic syndrome [2,3], neurodegenerative diseases [4], and some kinds of cancers [5]. Thus, anti-inflammation is thought to be beneficial and helpful for the prevention of these mentioned diseases. When inflammation occurs, iNOS and COX-2, key proteins in the inflammatory signaling pathway, are usually highly expressed, catalyzing to produce massive inflammatory cytokines including NO and PGE_2 [6]. Excessive inflammatory cytokines are considered to be a clear marker of inflammatory response, and inhibiting the production of these inflammatory cytokines becomes an appropriate anti-inflammatory strategy. In addition to synthetic small molecules used as anti-inflammatory agents to inhibit inflammation, natural products are also considered as an essential choice due to the structural and biological diversity and the potential value as lead compounds in drug development.

Casearia kurzii C. B. Clarke, belonging to the Flacourtiaceae plant family, is a small tree growing mainly in southern mainland of China [7]. Previous phytochemical studies on this plant and the other *Casearia* species revealed the major constituents of this genus to be terpenoids, phenylethanoids, flavonoids, phenolics, steroids, and volatile oils [8□34], which showed diverse biological effects [8]. While, some *Casearia* plants were employed historically as folk medicines in some countries, which attracted our attention on the bioactive components present in these plants. In our continuous search for bioactive natural products as potential anti-inflammatory agents or lead compounds for inflammatory disorders, caseahomopene A (**1**) with a ring-expanded homotriterpenoid skeleton (Fig. 1), was purified from the leaves of *C. kurzii*. Besides the structure elucidation, the anti-inflammatory effects of **1** were also examined to explore its application in drug development. We herein report the isolation, structural elucidation, as well as the anti-inflammatory effects in cell and zebrafish models.

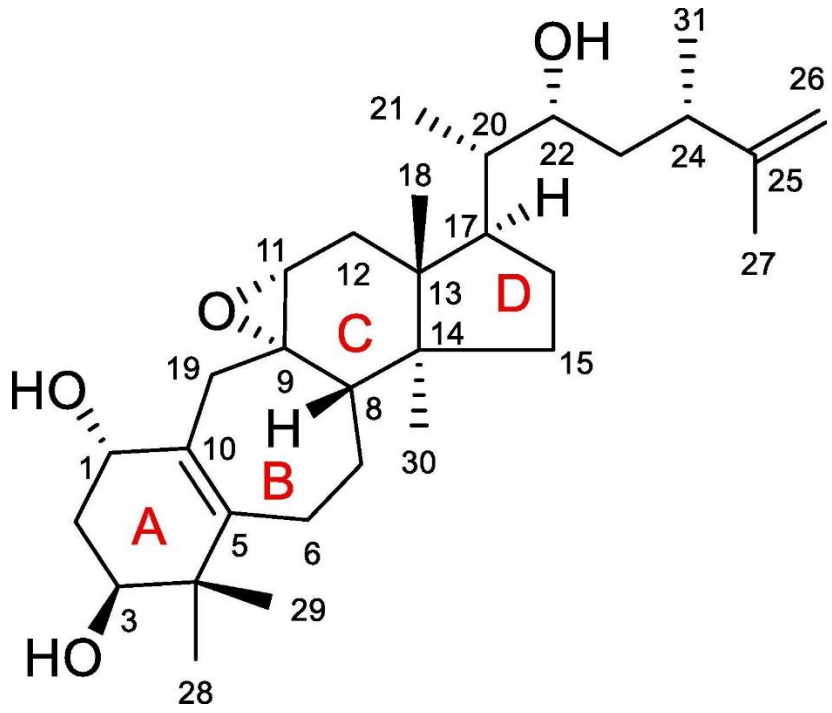

Fig. 1. Chemical structure of compound **1**.

2. Experimental Section

2.1. General experimental procedures

General experimental procedures were described in the Supplementary data.

2.2. Plant material

The leaves of *C. kurzii* were collected in May 2015 from Xishuangbanna, Yunnan Province, People's Republic of China. The botanical identification was made by one of the authors (Y. Guo), and a voucher specimen (No. 20150525X) was deposited in the Laboratory of Natural Medicinal Chemistry, Nankai University, People's Republic of China.

2.3. Extraction and isolation

The air-dried leaves of *C. kurzii* (14.0 kg) were extracted with MeOH (3 × 162 L) under reflux. The solvent was evaporated to afford a crude extract (3.1 kg). The extract was suspended in H_2O (3.1 L) and partitioned with petroleum ether and ethyl acetate successively. As a resulting residue, the EtOAc-soluble part (423.0 g) was subjected to a silica gel column chromatography eluted with petroleum

ether-acetone, to give eight fractions F_1□F_8 based on TLC analysis. Fraction F_7 was subjected to MPLC over ODS eluting with a step gradient from 65□95% MeOH in H_2O to give five subfractions F_{7-1}□F_{7-5}. The further purification of subfraction F_{7-3} by preparative HPLC on a YMC ODS-AM column (5 μm, 250 mm × 20 mm) using MeOH-H_2O (84: 16) as the mobile phase to yield **1** (t_R =40.0 min, 12.0 mg).

Caseahomopene A (**1**): colorless needles (MeOH); [α] −8.0 (*c* 0.3, CH_2Cl_2); IR (KBr) ν_{max} 3391, 2959, 2932, 1713, 1664, 1378, 1261, 1021, 801, 734 cm^{-1}; ^1H NMR (400 MHz, $CDCl_3$): δ_H 3.82 (1H, t, *J* = 3.5 Hz, H-1), 2.00 (1H, m, H-2〈), 1.72 (1H, m, H-2®), 3.86 (1H, dd, *J* = 11.6, 2.9 Hz, H-3), 2.50 (1H, m, H-6〈), 2.11 (1H, m, H-6®), 1.70 (1H, m, H-7〈), 1.30 (1H, m, H-7®), 1.66 (1H, overlapped, H-8), 3.15 (1H, t, *J* = 3.6 Hz, H-11), 2.01 (1H, d, *J* = 3.6 Hz, H-12〈), 1.93 (1H, d, *J* = 3.6 Hz, H-12®), 1.39 (1H, m, H-15〈), 1.31 (1H, m, H-15®), 1.80 (1H, m, H-16〈), 1.35 (1H, m, H-16®), 2.07 (1H, m, H-17), 0.80 (3H, s, H_3-18), 2.96 (1H, d, *J* = 14.2 Hz, H-19〈), 1.81 (1H, d, *J* = 14.2 Hz, H-19®), 1.50 (1H, m, H-20), 0.89 (3H, d, *J* = 6.4 Hz, H_3-21), 3.60 (1H, br d, *J* = 10.2 Hz, H-22), 1.36 (1H, m, H-23a), 1.27 (1H, m, H-23b), 2.44 (1H, m, H-24), 4.76 (2H, s, H_2-26), 1.64 (3H, s, H_3-27), 1.19 (3H, s, H_3-28), s, 0.91 (3H, s, H_3-29), 0.87 (3H, s, H_3-30), 1.06 (3H, d, *J* = 6.9, H_3-31); ^{13}C NMR (100 MHz, $CDCl_3$): δ_C 68.8 (C-1), 35.7 (C-2), 71.8 (C-3), 40.4 (C-4), 146.0 (C-5), 28.0 (C-6), 25.9 (C-7), 42.3 (C-8), 62.2 (C-9), 128.9 (C-10), 65.3 (C-11), 34.4 (C-12), 45.8 (C-13), 47.0 (C-14), 34.7 (C-15), 27.2 (C-16), 48.9 (C-17), 18.2 (C-18), 40.5 (C-19), 47.1 (C-20), 12.3 (C-21), 71.0 (C-22), 34.8 (C-23), 38.0 (C-24), 149.2 (C-25), 110.8 (C-26), 18.1 (C-27), 24.3 (C-28), 18.9 (C-29), 16.0 (C-30), 20.6 (C-31); ESIMS *m/z* 509 $[M + Na]^+$; HRESIMS *m/z* 509.3604 $[M + Na]^+$, calcd for $C_{31}H_{50}NaO_4$, 509.3607.

X-ray Crystal Data of caseahomopene A (**1**): $C_{31}H_{50}O_4$, M_r = 486.71, orthorhombic, space group *P*2(1)2(1)2(1), *a* = 11.30920 (10) Å, *b* = 14.24040 (10) Å, *c* = 18.2506 (2) Å, 〈 = 90°, ® = 90°, γ = 90°,*V* = 2939.21 (5) $Å^3$, *T* = 294 K, *Z* = 4, ⁄(Cu K〈) = 0.549 mm^{-1}, *D*calc = 1.100 g/cm^3, F(000) =1072, crystal dimensions 0.34 × 0.30 × 0.26 mm were used for measurements. The total number of reflections measured was 24223, of which 6138 were unique (*R*(int) = 0.0138). Final R_1 = 0.0295, wR_2 = 0.0837 ($I > 2\sigma(I)$), Flack parameter = □0.04 (3). Crystallographic data of this compound have been deposited

in the Cambridge Crystallographic Data Centre (CCDC 1957825).

2.4. Bioassay for NO production

The inhibition of NO was evaluated by inhibiting NO release in LPS-induced murine microglial BV-2 cells. The nitrite concentration in the culture supernatants was measured by Griess reaction according to the method described previously [35].

2.5. Bioassay for PGE_2 production

The PGE_2 production in the culture supernatant was measured using ELISA kits [36,37]. In brief, BV-2 cells were seeded in 24-well plates, treated with the test compound for 1 h, and then stimulated with LPS for 24 h. The cell supernatants were collected and used to detect PGE_2 levels according to the manufacturer's instructions.

2.6. Western blotting analysis

The Western blotting experiments were carried out as reported in the literature [38]. The detailed process was described in the the Supplementary data.

2.7. Molecular docking studies

The molecular docking studies were performed as described previously [39]. The three dimensional (3D) crystal structures of iNOS (PDB code: 3E6T) and COX-2 (PDB code: 1PXX) were obtained from the RCSB Protein Data Bank, whose resolution was 2.5 Å. The 3D structure of compound **1** was constructed by Chem3D software. Molecular docking simulations were carried out using the software AutoDock Vina along with AutoDock Tools (ADT 1.5.6).

2.8. Anti-inflammatory assay in vivo using zebrafish model

The production of NO and ROS in zebrafish embryos was detected by DAF-FMDA fluorescent probe dye and DCF-DA fluorescent probe dye, respectively [40]. Embryos were collected from adult

zebrafish as described previously [41]. Approximately 7 to 8 h post-fertilization (7-8 hpf), healthy embryos (15/group) were placed into 12 well culture plate and treated with or without the tested compounds. After 1 h, LPS (10 μg/mL) was added into the plate for a continuous incubation of 48 h at 28 °C. The embryos in 12-well plate were transferred to 24-well plate and treated with DCF-DA solution (20 μg/mL) for 1 h (for the measurement of ROS level) or DAF-FMDA (5 μM) for 2 h (for the measurement of NO level), both in dark at 28 ℃ [42]. Then, the embryos were washed with fresh embryo media and anesthetized, and a laser confocal microscope (Leica TCS SP8, Leica, Germany) was used to observe the stained embryos and photograph. The fluorescence intensity of individual zebrafish embryo was quantified using Image J software.

3. Results

3.1. Structure elucidation

Compound **1**, a colorless crystal (MeOH), gave a molecular formula $C_{31}H_{50}O_4$ according to its ^{13}C NMR data and the HRESIMS ion (*m*/*z* 509.3604 $[M + Na]^+$, calcd for $C_{31}H_{50}NaO_4$, 509.3607). The molecular formula displayed seven indices of hydrogen deficiency. The ^1H NMR spectrum displayed seven methyl signals assignable to four aliphatic methyl singlets (δ_H 0.80, 0.87, 0.91, and 1.19), two aliphatic methyl doublets [δ_H 0.89 (d, J = 6.4 Hz) and 1.06 (d, J = 6.9 Hz)], and one olefinic methyl singlet (δ_H 1.64). In addition, four oxymethine protons [δ_H 3.82 (1H, t, J = 3.5 Hz), 3.86 (1H, dd, J = 11.6, 2.9 Hz), 3.15 (1H, t, J = 3.6 Hz), and 3.60 (1H, br d, J = 10.2 Hz)] and two olefinic protons [δ_H 4.76 (2H, s)] were detected from its ^1H NMR spectrum. These spectroscopic features, especially the total seven methyl groups and numerous aliphatic carbons, suggested compound **1** to be a triterpenoid derivative [14,18,43□47], which was defined by the following HMBC and ^1H-^1H COSY experiments.

Analysis of the HMBC spectrum revealed the long range cross-peaks of H-1 to C-2, C-3, C-5, C-10, and C-19, and H_3-30 to C-8 and C-13□C-15, as well as the other crucial correlations depicted in Fig. 2. While, the ^1H-^1H COSY couplings of H-1/H_2-2/H-3, H_2-6/H_2-7/H-8, H_2-15/H_2-16/H-17/H-20/H-22/H_2-23/H-24/H_3-31, and the other correlations shown in Fig. 2, were also observed from the

^{1}H-^{1}H COSY spectrum of **1**. These HMBC and ^{1}H-^{1}H COSY data, along with the ^{1}H and ^{13}C NMR data, allowed the establishment of a 6/7/6/5 tetracyclic fused ring system, which carried four methyl groups (Me-18, Me-28, Me-29, and Me-30). Apart from this fused ring system, a side chain composed of C-20□C-27 and C-31 was deduced from ^{1}H-^{1}H COSY couplings of H_3-21/H-20/H-22/H_2-23/H-24/H_3-31 and the corresponding HMBC correlations illustrated in Fig. 2. This side chain was linked to C-17 of the 6/7/6/5 tetracyclic fused ring system by the HMBC correlations depicted in Fig. 2 and the key ^{1}H-^{1}H COSY coupling of H-17/H-20. All of the 1D and 2D NMR data analysis established a ring-expanded triterpenoid skeleton carrying an extra methyl (Me-31) attached at C-24, in which the four oxygenated carbons at δ_C 68.8, 71.8, 62.2, and 65.3 were assigned to C-1, C-3, C-9, and C-11. However, the chemical shifts of the oxygenated carbons C-9 and C-11 seemed to be upfield when compared to those oxygenated carbons of the ring. This clue, together with the HRESIMS data, disclosed the presence of a 9, 11-epoxy structural moiety. Thus, the 2D structure of compound **1** was determined as shown, which possesses a ring-expanded homotriterpenoid scaffold.

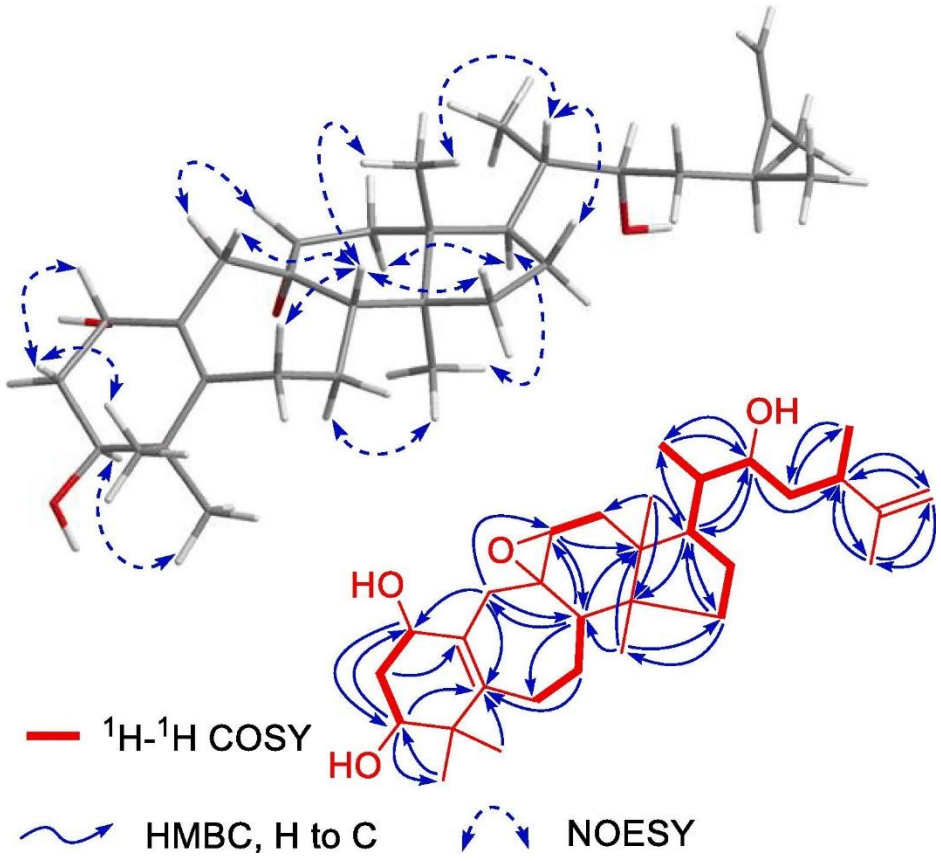

Fig. 2. Conformation, ^{1}H–^{1}H COSY, key HMBC, and crucial NOESY correlations of **1**.

A combination analysis of NOESY couplings, Chem3D modeling, and coupling constants was utilized to elucidate the spatial configuration. The NOESY spectrum of **1** showed the correlations of H-1/H-2⍺, H-2⍺/H_3-29, H-3/H_3-28, H-11/H_3-18, H-8/H_3-18, and H_3-30/H-17, as well as the other couplings depicted in Fig. 2. These NOE effects, along with Chem3D simulations, disclosed a conformation for **1** as shown in Fig. 2. In this steric conformation of **1**, rings B/C and C/D were *trans*-fused with H-8 and Me-18 in ⍺-positions and Me-30 in an ⍵-position. Ring A existed in a twist-chair conformation with H-1 ⍺-oriented and H-3 ⍵-oriented, as supported by the coupling constants of $J_{1,2\alpha/\beta}$ = 3.5 Hz and $J_{3,2\alpha/\beta}$ = 2.9, 11.6 Hz. Ring C presented a twist-chair conformation with the epoxy moiety on its ⍵-side, and ring D had an envelope conformation with H-17 on its ⍵-side. The C-20 configuration was deduced to be *rel*-20*S*, according to the corresponding correlations shown in Fig. 2. However, the configurations of the chiral carbons C-22 and C-24 were difficult to define due to the side chain flexibility.

Fortunately, the crystal of **1** in methanol was obtained and the X-ray diffraction analysis was thus performed, leading to the obtainment of the crystallography data of **1**. As shown in Fig. 3, an ORTEP drawing of **1** confirmed unambiguously the structure to be a homotriterpenoid derivative with a ring-expanded skeleton, and the absolute configuration was thus assigned as 3*S*, 8*S*, 9*S*, 11*R*, 13*R*, 14*S*, 17*R*, 20*S*, 22*R*, and 24*S* according to the Flack parameter [–0.04(3)].

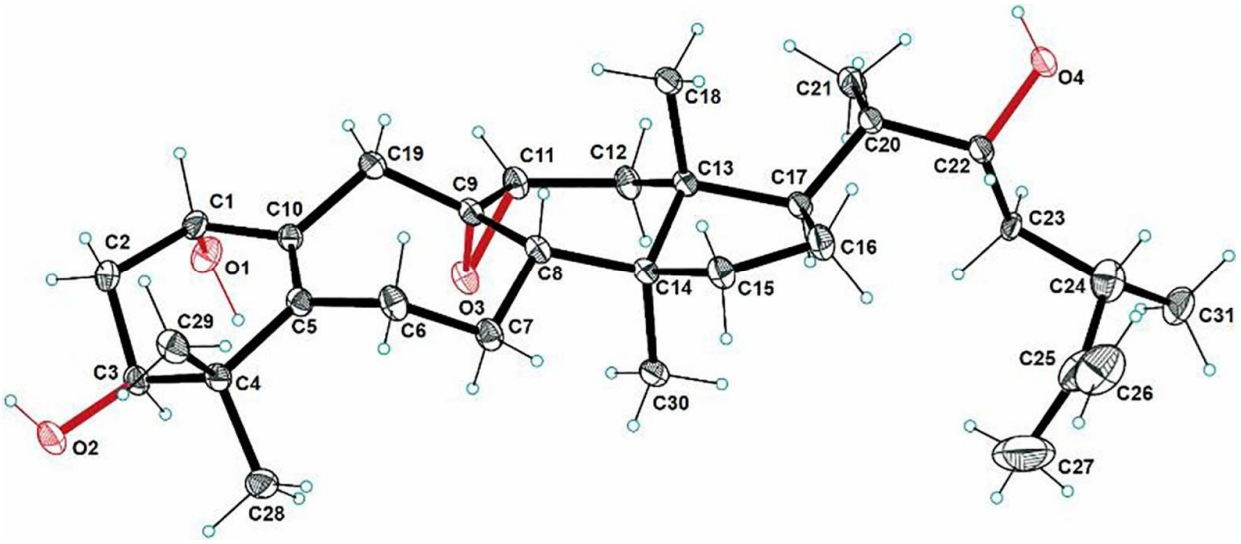

Fig. 3. ORTEP drawing of 1 by X-ray crystallographic diffraction analysis.

3.2. Anti-inflammatory effects of 1 on LPS-induced NO and PGE_2 production in BV-2 cells

To explore the potential medicinal application in drug development, a biological assay to evaluate the anti-inflammatory effects of **1** was carried out using LPS-induced BV-2 cells. In this model, NO and PGE_2, both which are inflammatory mediators and indictors of inflammatory response, were measured according to the method reported in the literature [48,49]. As shown in Fig. 4, compound **1** inhibited significantly NO production in LPS-stimulated BV-2 cells and gave an IC_{50} value of 8.9 μM, which is comparable to the positive control, 2-methyl-2-thiopseudourea, sulfate (SMT) (IC_{50} value, 1.6 μM). Besides NO production, the inhibitory effects for PGE_2 production were also detected, which revealed that compound **1** had the property of suppressing PGE_2 production with an IC_{50} value being 4.4 μM (IC_{50} value of SMT, 3.7 μM, Fig. 4). The results in cell level revealed that compound **1** to have promising anti-inflammatory effects by inhibiting inflammatory mediators NO and PGE_2.

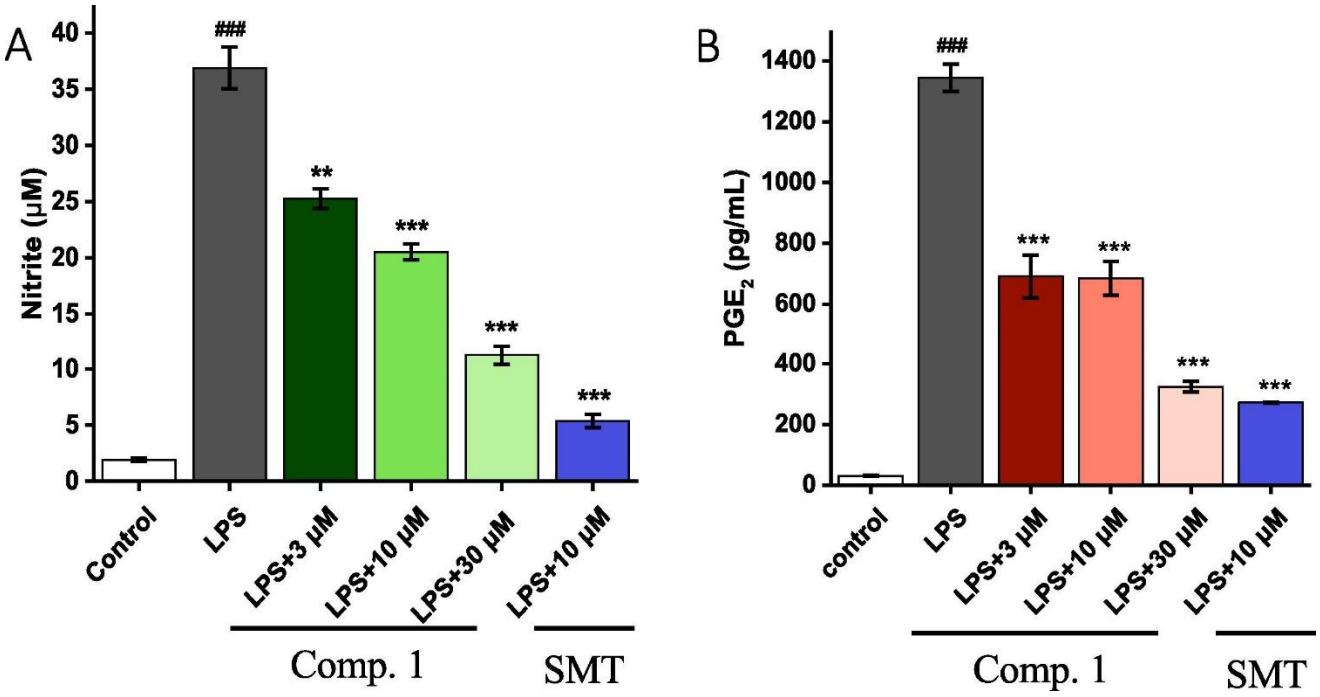

Fig. 4. Effects of compound **1** on LPS-induced NO and PGE_2 production in BV-2 cells. BV-2 cells were pretreated with compound **1** for 1 h, then the cells were exposed to LPS for 24 h, and production of NO and PGE_2 in cell free supernatants was tested. SMT was used as the positive control. (A) NO amount; (B) PGE_2 amount. Data were expressed as mean ± SD (n = 3). $^{###}P < 0.001$, significantly different from control; $^{**}P < 0.01$, $^{***}P < 0.001$, significantly different from LPS-treated sample.

3.3. Effects of compound 1 on LPS-induced iNOS and COX-2 expression in BV-2 cells

Compound **1** was found to have anti-inflammatory effects in LPS-induced BV-2 cells, which evoked our attention on its anti-inflammatory mechanism. When inflammation occurs, excessive inflammatory mediators such as NO and PGE_2, are released, which are catalyzed by iNOS and COX-2 enzymes, respectively [50,51]. The reduction of NO and PGE_2 production inhibited by compound **1**, means the decrease of the expression of two enzymes in the inflammatory signaling pathway. Thus, Western blotting experiments were performed to confirm whether the expressions of iNOS and COX-2 were decreased. As shown in Fig. 5, after stimulated by LPS for 24 h, the expressions of iNOS and COX-2 were increased remarkably. However, with the treatment of compound **1**, iNOS and COX-2 were decreased significantly. These results indicated that compound **1** may exert its anti-inflammatory effects by down-regulating iNOS and COX-2 protein levels.

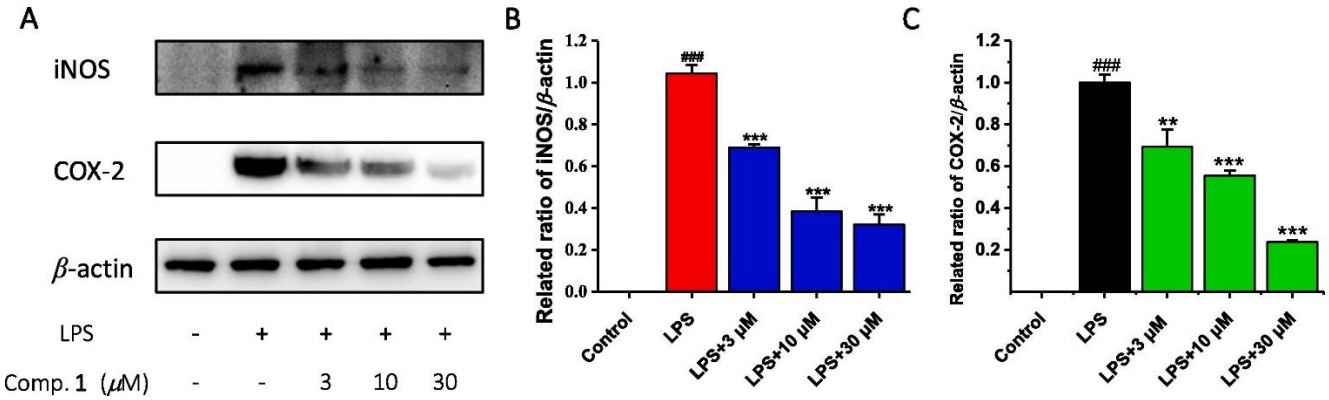

Fig. 5. Effects of compound **1** on LPS-induced iNOS and COX-2 expressions in BV-2 cells. BV-2 cells were pretreated with compound **1** for 30 min, then the cells were exposed to LPS for 20 h, western blotting analysis was then performed. (A) Western blotting; (B) iNOS expression; (C) COX-2 expression. Data were expressed as mean ± SD (n = 3). $^{###}P < 0.001$, significantly different from control; $^{**}P < 0.01$, $^{***}P < 0.001$, significantly different from LPS-treated sample.

3.4. Molecular docking simulations of 1 with iNOS and COX-2

Western blotting experiments displayed the down-regulation of iNOS and COX-2 proteins when treated by compound **1**. One possible mechanism for this down-regulation is the affinity binding of compound **1** with iNOS/COX-2 [52]. To under binding interactions of compound **1** with the two

proteins, molecular docking studies were applied to evaluate the binding ability and residues of compound **1** with iNOS/COX-2 [53,54]. As shown in Fig. 6, the docking results revealed that compound **1** had strong affinities with the iNOS/COX-2 protein, and the binding sites and logarithms of free binding energies of compound **1** were collated in Fig. 6. The affinity bindings between compound **1** and iNOS/COX-2 may cause the expression reduction of two proteins, which revealed the possible anti-inflammatory mechanism.

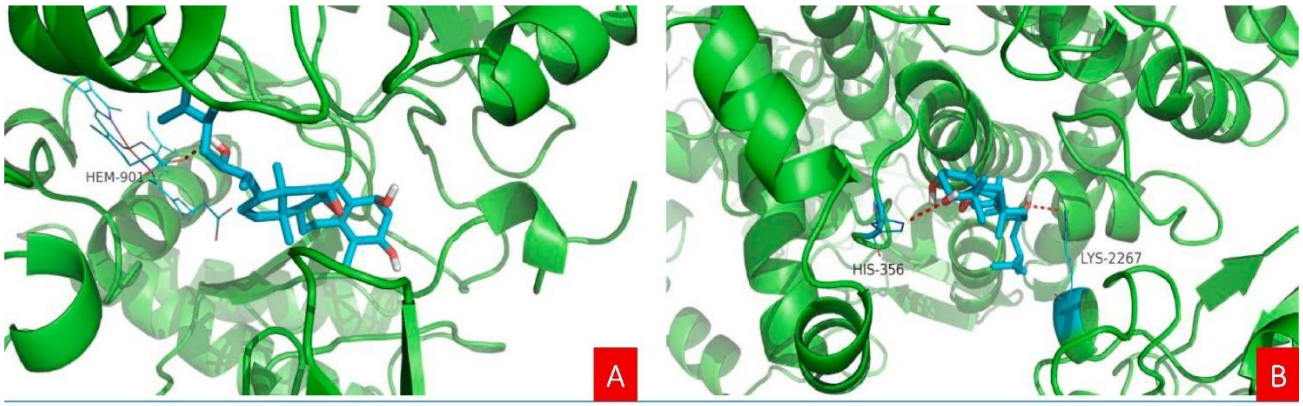

Protein	–Log (FBE)	Targeting residues
iNOS	–9.1	HEM-901
COX-2	–7.5	HIS-356 LYS-2267

Fig. 6. Molecular docking results of **1** with iNOS (A) and COX-2 (B). Molecular docking simulations obtained at the lowest energy conformation, highlighting potential hydrogen contacts, binding sites, and logarithms of free binding energy, respectively (Colored by atom: carbon is cyan; nitrogen is blue; oxygen is red; hydrogen is gray; sulfur is orange). For clarity, only interacting residues are labeled. Hydrogen bonding interactions are shown by dashes. These figures were created by PyMOL.

3.5. Effects of compound 1 on the production of ROS and NO in LPS-stimulated zebrafish embryos

Compound **1** exhibited strong anti-inflammatory activity *in vitro*, which evoked our great interest in its *in vivo* anti-inflammatory effects. Considering the inadequate amount of **1**, zebrafish model, an ideal animal experimental model used extensively for drug screening, was selected to evaluate the anti-inflammatory effects. In this *in vivo* assay model, inflammatory related mediators NO and ROS induced by LPS were released largely, whose levels were detected and considered as a sign of inflammatory degree [55,56]. As shown in Figs. 7 and 8, the amounts of ROS and NO production rose

significantly after stimulated by LPS. When treated with compound **1**, the ROS and NO production were reduced flowing the alternations of the concentration of **1**. The results of *in vivo* experiments showed that compound **1** had the property of inhibiting ROS and NO formation in a dose-dependent manner. The *in vivo* screening results revealed that compound **1** with strong anti-inflammatory effects is expected to be potentially useful for inflammatory diseases.

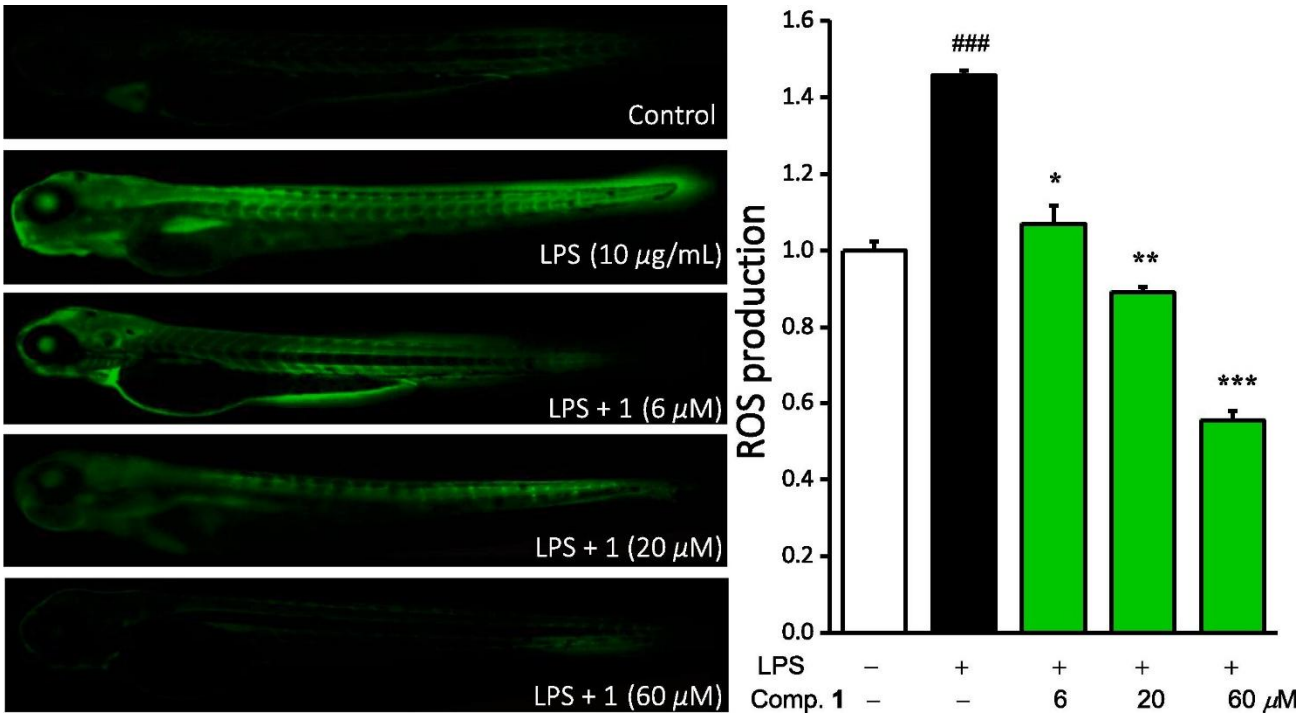

Fig. 7. Effects of compound **1** on the production of ROS in LPS-stimulated zebrafish embryos. Zebrafish embryos were stimulated by LPS (10 μg/mL) and treated with or without compound **1** (6, 20, and 60 μM) for 24 h. At 3 days post fertilization (dpf), the ROS levels were measured by laser confocal microscope. Fluorescence intensity was quantified using the Image J. Data were expressed as mean ± SD. $^{###}P < 0.001$ compared with LPS-untreated embryos; $^{***}P < 0.001$, $^{**}P < 0.01$, $^{*}P < 0.05$ compared with LPS-stimulated embryos.

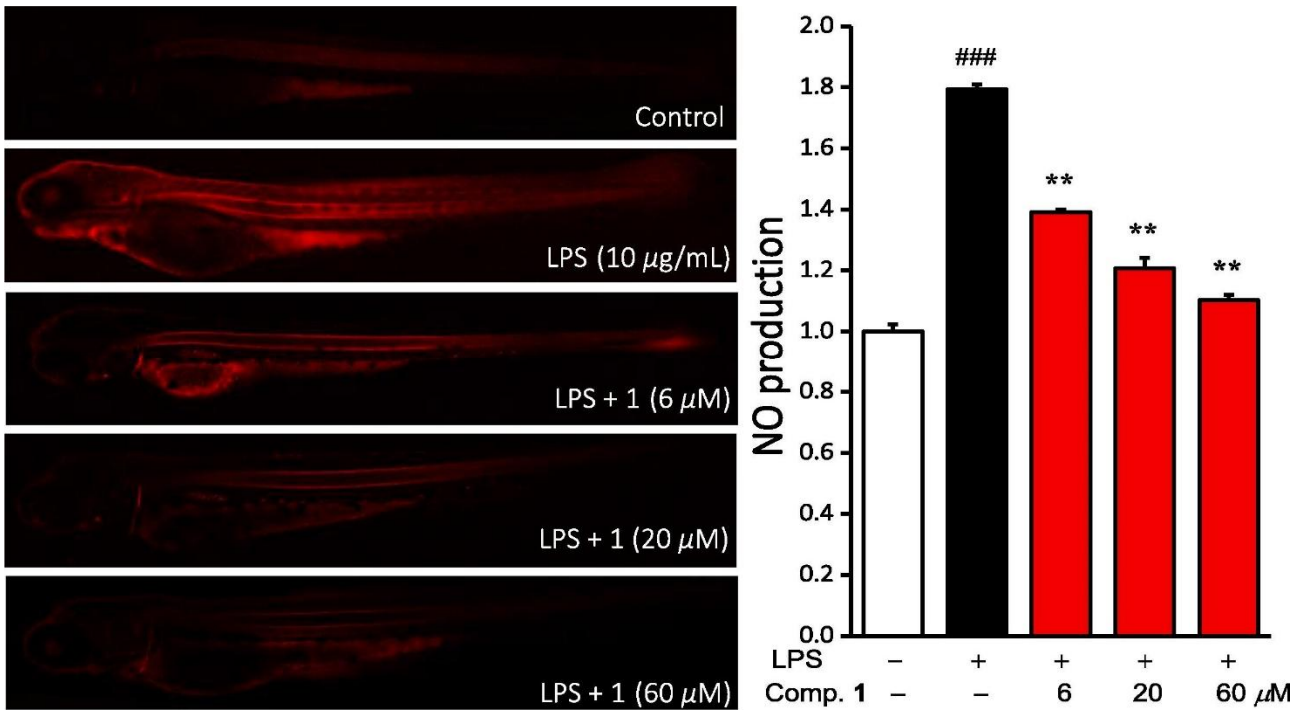

Fig. 8. Effects of compound **1** on production of NO in LPS-stimulated zebrafish embryos. Zebrafish embryos were stimulated by LPS (10 μg/mL) with or without compound **1** (6, 20, and 60 μM) for 24 h. At 3 days post fertilization (dpf), the NO levels were measured by laser confocal microscope. Fluorescence intensity was quantified using the Image J. Data were expressed as mean ± SD. $^{###}P < 0.001$ compared with LPS-untreated embryos, $^{**}P < 0.01$, compared with LPS-stimulated embryos.

4. Discussion

As part of our search for bioactive natural products as lead compounds for the treatment of inflammatory disorders, a triterpenoid derivative was obtained from the leaves of *C. kurzii*. The 1D and 2D NMR experiments were performed and the NMR data obtained were employed to establish the 2D structure, which is a novel triterpenoid derivative with a ring-expanded homotriterpenoid skeleton. Besides the relative configuration deduced from the NMR data, the absolute configuration of **1** was determined using X-ray diffraction analysis, which was finally defined as being a novel triterpenoid derivative with a ring-expanded homotriterpenoid skeleton. To the best of our knowledge, ring-expanded homotriterpenoids are reported to be rare in nature [14,18].

Natural products play an important role in the development of new drugs and numerous new drugs have been derived from natural products. Compound **1**, elucidated as a novel triterpenoid derivative

with a ring-expanded homotriterpenoid skeleton, attracted our attention to its biological activities and the exploration of medicinal potential. The pathogenesis of numerous diseases is related to inflammation, so the anti-inflammatory assay was performed. When inflammation happens, a large number of NO and PGE_2 are released, while the up-stream regulated proteins iNOS and COX-2 are highly expressed. When inflammatory response is inhibited by active molecules, the amounts of NO and PGE_2 are usually reduced and the expression levels of the proteins iNOS and COX-2 are decreased. In our cell experiments, compound **1** inhibited NO (IC_{50}, 8.9 μM) and PGE_2 (IC_{50}, 4.4 μM) production, and the Western blotting results showed that the expressions of iNOS and COX-2 were down-regulated. These experiments confirmed unambiguously the anti-inflammatory effects of **1**. Considering the possible mechanism of iNOS and COX-2 down-regulation being the affinity bindings, molecular docking was further employed to predict the binding ability and sites of compound **1** with iNOS/COX-2, which exhibited the strong interactions between **1** with the residues of iNOS/COX-2.

As a bioactive compound, **1** showed promising activities in cell level, drawing our interest in its *in vivo* biological effects. However, it is difficult to conduct mouse experiment due to the limit of the amount of **1**. Zebrafish, as a living being highly homologous to human, is an ideal model for drug screening. In this *in vivo* zebrafish model, a large amount of NO and ROS produced by treatment with LPS, which were a sign of inflammatory response. After treated with compound **1** (6, 20, and 60 μM), the production of NO decreased by 22%, 33%, and 38%, respectively. The other indicator ROS of inflammatory response degree, was also detected, whose level was also significantly decreased when treated by compound **1**. The *in vivo* biological experiments implied that compound **1** is potentially useful for inflammatory diseases.

5. Conclusions

In this study, a rare natural product with a ring-expanded homotriterpenoid skeleton, caseahomopene A, was purified from the leaves of *C. kurzii*. The structure including the absolute configuration was determined by spectroscopic data and X-ray crystallography analysis. Compound **1** exhibited promising anti-inflammatory effects, whose possible action mechanism is to regulate the up-stream

protein levels of iNOS and COX-2 and bind some residues of iNOS and COX-2. The zebrafish experiments revealed compound **1** to have anti-inflammatory activity *in vivo*. All of the results disclosed that compound **1** is expected to be potential useful for the development of new anti-inflammatory drugs.

Conflict of interest

The authors of the present manuscript have declared that no competing interests exist.

Acknowledgments

This research was supported financially by the National Key Research and Development Program of China (No. 2018YFA0507204), the National Natural Science Foundation of China (Nos. U1703107 and U1801288), the Natural Science Foundation of Tianjin, China (No. 19JCYBJC28100), Hundred Young Academic Leaders Program of Nankai University, State Key Laboratory of Bioactive Substance and Function of Natural Medicines (Institute of Materia Medica, Chinese Academy of Medical Sciences and Peking Union Medical College, No. GTZK201902), and the open project of Key Laboratory of Xinjiang Uygur Autonomous Region (Nos. 2015KL030 and 2017D04019).

Conflicts of Interest: The authors declare no competing financial interest.

References

[1] Y. Zhu, X. Xian, Z. Wang, Y. Bi, Q. Chen, X. Han, D. Tang, R. Chen, Biomolecules 8 (2018) E80.

[2] N. Esser, S. Legrand-Poels, J. Piette, A.J. Scheen, N. Paquot, Diabetes Res. Clin. Pract. 105 (2014) 141□150.

[3] E. Lontchi-Yimagou, E. Sobngwi, T.E. Matsha, A.P. Kengne, Curr. Diab. Rep. 13 (2013) 435□444.

[4] J. Stephenson, E. Nutma, P. van der Valk, S. Amor, Immunology 154 (2018) 204□219.

[5] L.M. Coussens, Z. Werb, Nature 420 (2002) 860□867.

[6] T.K. Lee, T.A. Trinh, S.R. Lee, S. Kim, H.M. So, E. Moon, G.S. Hwang, K.S. Kang, J.H. Kim, N. Yamabe, K.H. Kim, Bioorg. Chem. 82 (2019) 26□32.

[7] Editorial Committee of the Flora of China, Chinese Academy of Sciences. Flora of China, Science Press, Beijing, Vol.52 (1), 1999, 69−72.

[8] L. Xia, Q. Guo, P.F. Tu, X.Y. Chai, Phytochemistry Reviews 14 (2015) 99−135.

[9] F.B. Oda, E.J. Crevelin, A.E.M. Crotti, A.B. Orlando, A.I. de Medeiros, F.A.R. Nogueira, A.G. Dos Santos, Fitoterapia 137 (2019) 104197.

[10] S. Yuan, C. Zhang, X. Yang, F. Liu, Q. Zhang, Li. An, J. Ma, D. Lee, Y. Ohizumi, Y. Guo, J. Nat. Med. 73 (2019) 826−833.

[11] F. Liu, Q. Zhang, X. Yang, Y. Xi, X. Zhang, H. Wang, J. Zhang, M. Tuerhong, D.Q. Jin, D. Lee, J. Xu, Y. Ohizumi, L. Shuai, Y. Guo, Bioorg. Chem. 89 (2019) 102995.

[12] J. Ma, X. Yang, Q. Zhang, X. Zhang, C. Xie, M. Tuerhong, J. Zhang, D.Q. Jin, D. Lee, J. Xu, Y. Ohizumi, Y. Guo, Bioorg. Chem. 85 (2019) 558−567.

[13] A.L. Santos, E.S. Yamamoto, L.F.D. Passero, M.D. Laurenti, L.F. Martins, M.L. Lima, M. Uemi, M.G. Soares, J.H.G. Lago, A.G. Tempone, P. Sartorelli, Chem. Biodivers. 14 (2017) e1600458.

[14] J. Xu, J. Kang, X. Sun, X. Cao, K. Rena, D. Lee, Q. Ren, S. Li, Y. Ohizumi, Y. Guo, J. Nat. Prod. 79 (2016) 170−179.

[15] H.T. Nguyen, N.B. Truong, H.T. Doan, M. Litaudon, P. Retailleau, T.T. Do; H.V. Nguyen, M.V. Chau, C.V. Pham, J. Nat. Prod. 78 (2015) 2726−2730.

[16] J. Xu, F. Ji, X. Sun, X. Cao, S. Li, Y. Ohizumi, Y. Guo, J. Nat. Prod. 78 (2015) 2648−2656.

[17] J. Xu, Q. Zhang, M. Wang, Q. Ren, Y. Sun, D.Q. Jin, C. Xie, H. Chen, Y. Ohizumi, Y. Guo, J. Nat. Prod. 77 (2014) 2182−2189.

[18] B. Wang, X.L. Wang, S.Q. Wang, T. Shen, Y.Q. Liu, H. Yuan, H.X. Lou, X.N. Wang, J. Nat. Prod. 76 (2013) 1573−1579.

[19] D.D. Bou, J.H. Lago, C.R. Figueiredo, A.L. Matsuo, R.C. Guadagnin, M.G. Soares, P. Sartorelli, Molecules 18 (2013) 9477−9487.

[20] M. Ismail, G. Bagalkotkar, S. Iqbal, H.A. Adamu, Molecules 17 (2012) 5745−5756.

[21] K.O. Rayanil, C. Nimnoun, P. Tuntiwachwuttikul, Phytochem. Lett. 5 (2012) 59−62.

[22] G.M. Vieira-Júnior, L.A. Dutra, P.M. Ferreira, M.O. de Moraes, L.V. Costa Lotufo, Cdo.Ó. Pessoa, R.B. Torres, N. Boralle, Vda.S. Bolzani, A.J. Cavalheiro, J. Nat. Prod. 74 (2011) 776−781.

[23] E.L. Whitson, C.L. Thomas, C.J. Henrich, T.J. Sayers, J.B. McMahon, T.C. McKee, J. Nat. Prod. 73 (2010) 2013–2018.

[24] W. Wang, Z. Ali, X.C. Lia, I.A. Khan, Nat. Prod. Commun. 5 (2010) 771−774.

[25] X.Y. Chai, F.F. Li, C.C. Bai, Z.R. Xu, H.M. Shi, P.F. Tu, Planta Med. 76 (2010) 91−93.

[26] A.G. dos Santos, P.M. Ferreira, G.M. Vieira Júnior, C.C. Perez, A. Gomes Tininis, G.H. Silva, S. Bolzani Vda, L.V. Costa-Lotufo, O. Pessoa Cdo, A.J. Cavalheiro, Chem. Biodivers. 7 (2010) 205−215.

[27] W. Wang, Z. Ali, X.C. Li, I.A. Khan, Helv. Chim. Acta 93 (2010) 139−146.

[28] W. Wang, J. Zhao, Y.H. Wang, T.A. Smillie, X.C. Li, I.A. Khan, *Planta. Med. 75* (2009) 1436−1441.

[29] W. Wang, Z. Ali, X.C. Li, I.A. Khan, Helv. Chim. Acta. 92 (2009) 1829−1839.

[30] G.M.J. Vieira, T.O. Gonçalves, L.O. Regasini, P.M. Ferreira, C.O. Pessoa, L.L.V. Costa, R.B. Torres, N. Boralle, V.S. Bolzani, A.J. Cavalheiro, J. Nat. Prod. 72 (2009) 1847–1850.

[31] W. Wang, Z. Ali, X.C. Li, T.A. Smillie, D.A. Guo, I.A. Khan, Fitoterapia 80 (2009) 404−407.

[32] W. Wang, X.C. Li, Z. Ali, I.A. Khan, Chem. Pharm. Bull. 57 (2009) 636−638.

[33] S.L. Da Silva, J.D.S. Chaar, T. Yano, Eur. J. Pharmacol. 608 (2009) 76−83.

[34] S. Kanokmedhakul, K. Kanokmedhakul, M. Buayairaksa, J. Nat. Prod. 70 (2007) 1122−1126.

[35] Y. Liang, L. An, Z. Shi, X. Zhang, C. Xie, M. Tuerhong, Z. Song, Y. Ohizumi, D. Lee, L. Shuai, J. Xu, Y. Guo, J. Nat. Prod. 82 (2019) 1634□1644.

[36] J.S. Lee, M. Jeong, S. Park, S.M. Ryu, J. Lee, Z. Song, Y. Guo, J.-H. Choi, D. Lee, D.S. Jang, Biomolecules 9 (2019) 806.

[37] H. Wang, Y. Liu, J. Zhang, J. Xu, C.A. Cui, Y. Guo, D.Q. Jin, Neurosci. Lett. 612 (2016) 149–154.

[38] S.R. Lee, S. Lee, E. Moon, H.J. Park, H.B. Park, K.H. Kim, Bioorg. Chem. 70 (2017) 94–99.

[39] P. Wang, X. Yang, F. Liu, Y. Liang, G. Su, M. Tuerhong, D.Q. Jin, J. Xu, D. Lee, Y. Ohizumi, Y. Guo, Bioorg. Chem. 76 (2018) 53–60.

[40] I.P.S. Fernando, K.K.A. Sanjeewa, K.W. Samarakoon, W.W. Lee, H.S. Kim, N. Kang, P. Ranasinghe, H.S. Lee, Y.J. Jeon, Int. J. Biol. Macromol. 104 (2017) 1185–1193.

[41] Y. Sun, G. Zhang, Z. He, Y. Wang, J. Cui, Y. Li, Int. J. Nanomed. 11 (2016) 905□918.

[42] E.Y. Ko, S.J. Heo, S.H. Cho, W. Lee, S.Y. Kim, H.W. Yang, G. Ahn, S.H. Cha, S.H. Kwon, M.S. Jeong, K.P. Lee, Y.J. Jeon, K.N. Kim, Int. Immunopharmacol. 67 (2019) 98–105.

[43] Y.C. Shen, Y.B. Cheng, A.F. Ahmed, C.L. Lee, S.Y. Chen, C.T. Chien, Y.H. Kuo, G.L. Tzeng, J. Nat. Prod. 68 (2005) 1665–1668.

[44] S. Kanokmedhakul, K. Kanokmedhakul, T. Kanarsa, M. Buayairaksa,. J. Nat. Prod. 68 (2005) 183−188.

[45] C.V. Sai Prakash, J.M. Hoch, D.G. Kingston, J. Nat. Prod. 65 (2002) 100−107.

[46] T.B. Chen, D.F. Wiemer, J. Nat. Prod. 54 (1991) 1612−1618.

[47] R.B. Williams, A. Norris, J.S. Miller, C. Birkinshaw, F. Ratovoson, R. Andriantsiferana, V.E. Rasamison, D.G. Kingston, J. Nat. Prod. 70 (2007) 206−209.

[48] P.S. Mishra, K. Vijayalakshmi, A. Nalini, T.N. Sathyaprabha, B.W. Kramer, P.A. Alladi, T.R. Raju, J. Neuroinflam. 16 (2017) 251□268.

[49] L. An, Y. Liang, X. Yang, H. Wang, J. Zhang, M. Tuerhong, D. Li, C. Wang, D. Lee, J. Xu, L. Shuai, J. Jin, Y. Guo, Bioorg. Chem. 92 (2019) 103237.

[50] C.H. Yu, B. Suh, I. Shin, E.H. Kim, D. Kim, Y.J. Shin, S.Y. Chang, S.H. Baek, H. Kim, O.N. Bae, Int. J. Mol. Sci. 20 (2019) 2607.

[51] E. Bakondi, S.B. Singh, Z. Hajnády, M. Nagy-Pénzes, Z. Regdon, K. Kovács, C. Hegedűs, T. Madácsy, J. Maléth, P. Hegyi, M.Á. Demény, T. Nagy, S. Kéki, É. Szabó, L. Virág, Int. J. Mol. Sci. 20 (2019) 4308.

[52] E.D. Garcin, A.S. Arvai, R.J. Rosenfeld, M.D. Kroeger, B.R. Crane, G. Andersson, G. Andrews, P.J. Hamley, P.R. Mallinder, D.J. Nicholls, S.A. St-Gallay, A.C. Tinker, N.P. Gensmantel, A. Mete, D.R. Cheshire, S. Connolly, D.J. Stuehr, A. Aberg, A.V. Wallace, J.A. Tainer, E.D. Getzoff, Nat. Chem. Biol. 4 (2008) 700□707.

[53] L. Ma, C. Xie, Y. Ma, J. Liu, M. Xiang, X. Ye, H. Zheng, Z. Chen., Q. Xu, T. Chen, J. Chen, J. Yang, N. Qiu, G. Wang, X. Liang, A. Peng, S. Yang, Y. Wei, J. Chen, J. Med. Chem. 54 (2011) 2060□2068.

[54] D. Tang, Y.Z. Xu, W.W. Wang, Z. Yang, B. Liu, M. Stadler, L.L. Liu, J.M. Gao, J. Nat. Prod. 82 (2019) 1599□1608.

[55] E.Y. Ko, S.J. Heo, S.H. Cho, W. Lee, S.Y. Kim, H.W. Yang, G. Ahn, S.H. Cha, S.H. Kwon, M.S. Jeong, K.P. Lee, Y.J. Jeon, K.N. Kim, Int. Immunopharmacol. 67 (2019) 98□105.

[56] E.A. Kim, S.Y. Kim, B.R. Ye, J. Kim, S.C. Ko, W.W. Lee, K.N. Kim, I.W. Choi, W.K. Jung, S.J. Heo, Int. Immunopharmacol. 59 (2018) 339□346.